

## *Electrochemical Behavior of Copper Electrodes Modified with CS-GA-ZnO Np/Polysulfone Nanocomposites via Cyclic Voltammetry*

Delinda Nirmala Afiyah<sup>1,2</sup>, Arie Hadian<sup>1,2</sup>, Anceu Murniati<sup>1,2,\*</sup>

<sup>1</sup>Department of Chemistry, Faculty of Sciences and Informatics (FSI), University of Jenderal Achmad Yani, Cimahi, Indonesia

<sup>2</sup>Material and Environmental Development Center, Universitas Jenderal Achmad Yani (Unjani), Cimahi, Indonesia

\*E-mail: [anceu.murniati@lecture.unjani.ac.id](mailto:anceu.murniati@lecture.unjani.ac.id)

DOI: <https://doi.org/10.26874/jkk.v8i1.932>

Received: 30 May 2025, Revised: 30 Juni 2025, Accepted: 30 Juni 2025, Online: 1 Juli 2025

### *Abstract*

Copper (Cu) is an economical alternative electrode material with high electrical conductivity and electrochemical properties that support redox reactions. To enhance its electrochemical performance, the copper electrode was modified using a nanocomposite consisting of 5% chitosan (CS), 5% polysulfone (Psf), 0.9% Zinc Oxide nanoparticles (ZnO Np), and 25% glutaraldehyde (GA). This study aims to characterize and evaluate the electrochemical performance of the CS-GA-ZnO NP/Psf-modified copper electrode using cyclic voltammetry and FTIR spectroscopy. Cyclic voltammetry characterization was carried out using 0.03 M  $K_3[Fe(CN)_6]$  and 0.01 M analytical-grade glucose solutions, both prepared in 0.1 M KCl, with scan rate variations of 15–30 mV/s. The optimum scan rate for the  $K_3[Fe(CN)_6]$  solution was found to be 20 mV/s with an oxidation-to-reduction current ratio ( $I_{pa}/I_{pc}$ ) of 1.01, while for glucose, the optimum scan rate was 30 mV/s with a ratio of 0.74. The FTIR spectrum showed a peak at 1643  $cm^{-1}$ , indicating successful crosslinking between chitosan and glutaraldehyde through the formation of imine bonds (CH=N). These findings demonstrate that the CS-GA-ZnO NP/Psf nanocomposite effectively enhances electron transfer efficiency on the copper electrode surface. This modified electrode shows strong potential for application in electrochemical sensors, particularly for glucose detection.

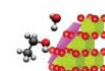
**Keywords:** Copper, Cyclic voltammetry, FTIR, Modified electrode, Nanocomposite

### **1 Introduction**

The development of electrochemical sensor technology continues to advance to enhance sensitivity, selectivity, and stability. One innovative strategy involves the modification of electrodes using nanocomposite materials, such as copper electrodes modified with chitosan, glutaraldehyde, zinc oxide nanoparticles (ZnO Np), and polysulfone. Copper is selected as an alternative electrode material due to its low cost, excellent electrical conductivity, and favorable redox properties. Surface modification using nanocomposites is expected to significantly improve the stability and electrochemical performance of copper electrodes [1].

The nanocomposite utilized in this study integrates four key components: chitosan (CS), glutaraldehyde (GA), ZnO Np, and polysulfone

(Psf). Chitosan, a biocompatible and biodegradable biopolymer, serves as the main matrix due to its film-forming ability and chemical functionality, although it exhibits low intrinsic electrical conductivity [2][3]. To enhance electron transfer rates, ZnO nanoparticles are introduced, as they possess high surface area, favorable conductivity, and catalytic activity, making them suitable for improving electron mobility in sensing applications [4–6]. Polysulfone is added to strengthen the mechanical properties and thermal stability of the nanocomposite, ensuring long-term durability under operational conditions. The addition of glutaraldehyde serves to crosslink the chitosan matrix, forming imine bonds that increase structural compactness and stability [7][8]. Prior research [6] has shown that adjusting the concentration of chitosan significantly affects



electrode sensitivity, indicating the need to optimize nanocomposite composition for maximum performance.

Electrochemical performance was evaluated via cyclic voltammetry, revealing redox activity and electrode stability. Prior studies [9, 10] highlight electrode modification potential. This study integrates functional materials to develop a stable, efficient, and low-cost electrochemical sensor for practical applications.

## 2 Method

### 1.1 Material

The materials used in this study were of pro-analytical grade to ensure accuracy and consistency of the results. The primary materials included chitosan (CS) extracted from blue crab shells (*Rajungan/P. pelagicius*) with a particle size of 200-300 mesh, Zinc acetate dihydrate ( $\text{Zn}(\text{CH}_3\text{COO})_2 \cdot 2\text{H}_2\text{O}$ ,  $\geq 99\%$ , HmbG Chemicals) as precursor, Sodium hydroxide (NaOH,  $\geq 98\%$ , Sigma-Aldrich) as alkaline agent, Absolute ethanol and distilled water as solvent media, glutaraldehyde ( $\text{OHC}(\text{CH}_2)_3\text{CHO}$ ) 25% from Merck, glacial acetic acid ( $\text{CH}_3\text{COOH}$ ) 100% from Merck, polysulfone ( $[\text{C}_6\text{H}_4\text{-4-C}(\text{CH}_3)_2\text{C}_6\text{H}_4\text{-4-O}]_n$ ), N-Methyl-2-pyrrolidone (NMP). Additional materials used included potassium chloride (KCl), potassium ferricyanide [ $\text{K}_3\text{Fe}(\text{CN})_6$ ], glucose ( $\text{C}_6\text{H}_{12}\text{O}_6$ ), distilled water (aquabidest), and copper wire (Cu).

### 1.2 Instrumentation

Instruments used included standard chemical glassware, a magnetic stirrer, capillary tubes, an analytical balance, a platinum electrode (Pt), an Ag/AgCl electrode, and INGENS<sup>TM</sup> Electrochemical Workstation potentiostat (Type 1030), and a laptop for data processing. These materials and instruments supported the synthesis, modification, and characterization processes effectively [11].

### 1.3 In Situ Synthesis of ZnO nanoparticles via the Sol-Gel Method

ZnO nanostructures were synthesized via sol-gel method using zinc acetate dihydrate (precursor) dissolved in ethanol/water (3:1 v/v). NaOH solution (0.5M) was added dropwise under stirring at 70°C to form a gel, which was aged for 24h. The product was dried (80°C, 12h) and calcined (450°C, 2h). This method produced crystalline ZnO nanostructures with controlled morphology, confirmed by XRD and SEM characterization. [12].

### 1.4 Synthesis of CS-GA-ZnO Np/Psf Nanocomposite

A 5% chitosan (CS) solution was mixed with 0.9% ZnO nanoparticles (NPs) under heated stirring to ensure homogeneity. Glutaraldehyde (25% GA) was then added to crosslink the CS-ZnO mixture, followed by incorporation of 5% polysulfone (PSf) under controlled heating to form a uniform paste.

The optimized concentrations (5% CS, 5% PSf, 0.9% ZnO NPs, 25% GA) were determined through systematic studies. The 5% CS balances viscosity and amino group availability, while 0.9% ZnO NPs provide optimal surface area without aggregation. The 25% GA ensures effective crosslinking without excessive rigidity, and 5% PSf enhances mechanical stability while maintaining conductivity [5].

### 1.5 Preparation of Modified Copper Electrodes with CS-GA-ZnO Np/Psf

Copper wire was cut into length of 7 cm with a diameter of approximately  $\pm 2$  mm. The surface of the copper wire was then polished using sandpaper with progressively finer grits. Subsequently, the copper electrode was thoroughly washed with deionized water to remove any remaining abrasive particles. Once clean and dry, the electrode was inserted into a capillary tube to facilitate the coating process. The copper electrode was then dipped into the CS-GA-ZnO/Psf nanocomposite pasta using the dip-coating method.

### 1.6 Characterization of Modified Copper Electrode with CS-GA-ZnO Np/Psf

Electrochemical performance of the CS-GA-ZnO Np/Psf working electrode was evaluated using cyclic voltammetry and infrared (IR) spectroscopy. The analyte solutions included 0.03 M potassium ferricyanide and 0.01 M p.a.-grade glucose, both prepared in 0.1 M KCl. Voltammograms were recorded over a potential range of -2.0 to 0.80 V (ferricyanide) and -3.5 to 2.0 V (glucose) at scan rates of 15, 20, 25, and 30 mV/s. These scan rates were selected based on previous research demonstrating their effectiveness in evaluating redox kinetics [5].

The infrared (IR) spectroscopy was analyzed using the FTIR Prestige 21 from Shimadzu to identify functional groups and confirm nanocomposite formation. The analyzed samples included chitosan, glutaraldehyde, polysulfone, and the CS-GA-ZnO Np/Psf nanocomposite in both liquid and solid film forms.

### 3 Result and Discussion

#### 3.1 Synthesis and Preparation of CS-GA-ZnO Np/Psf Nanocomposite for Modified Copper Electrode

The CS-GA-ZnO Np/Psf nanocomposite film was prepared by mixing chitosan, glutaraldehyde, ZnO nanoparticles (Np), and polysulfone. Initially, a (5%) chitosan solution was mixed with a (0,9%) ZnO Np solution pre-dissolved in 1% glacial acetic acid under stirring and heating at a temperature of 50-60 °C [5]. both chitosan and ZnO Np are insoluble in water but dissolve in organic acids such as acetic acid [4]. During the mixing process, the viscosity of the solution decreased due to hydrolysis between chitosan and glacial acetic acid. Chitosan contains hydroxyl and amine groups capable of forming hydrogen bonds both intermolecularly and intramolecularly. The longer the contact time between chitosan and glacial acetic acid, the greater the number of hydrogen bonds formed, especially between the hydrogen of the amine group in chitosan and the hydrogen of acetic acid [13].

Chitosan, although a biopolymer, has low conductivity and was therefore combined with

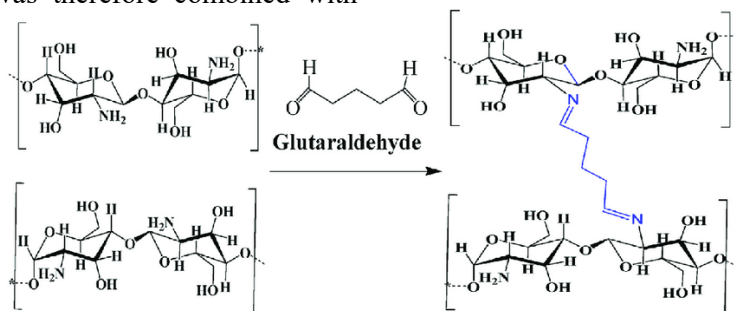


Figure 1 Crosslinking Mechanism of Chitosan with Glutaraldehyde [16]

The coating of the copper working electrode with a CS-GA-ZnO Np/Psf nanocomposite film was performed using the dip-coating method. The tip of the electrode was dipped into the nanocomposite film paste until its surface was evenly coated, followed by drying for at least 6 hours before being used for cyclic voltammetry measurements. The length and diameter of the electrode was 5 cm and 0.2 cm, respectively (Fig. 2).

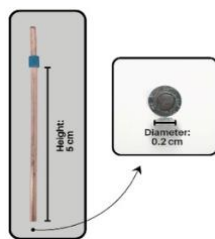


Figure 2 Working electrode modified with CS-GA-ZnO Np/Psf nanocomposite

ZnO Np to enhance the conductivity and surface area of the electrochemical sensor [4]. Conductivity is a critical factor in electrode sensors, ensuring efficient electron transfer between the electrode and the analyte solution, thus improving the sensitivity and accuracy of electrochemical measurements [6].

Subsequently, glutaraldehyde (25%) was added to the chitosan-ZnO Np mixture as a crosslinking agent to improve the mechanical strength, stability, and permeability of the nanocomposite film. Crosslinking is essential because pure chitosan is brittle and has low mechanical strength, particularly in thin or dry film form [14]. The crosslinking process occurs when free amine groups (-NH<sub>2</sub>) in chitosan react with aldehyde groups (-CHO) in glutaraldehyde through a nucleophilic reaction, forming a covalent Schiff Base (-C=N-) or imine bond. This reaction (Fig. 1) involves a nucleophilic attack by the lone electron pair on the amine group towards the electrophilic carbon atom of the aldehyde group, followed by the release of a water molecule (H<sub>2</sub>O) [15][16].

#### 3.2 Characterization of CS-GA-ZnO Np/Psf-Modified Copper Electrodes Using Cyclic Voltammetry

Cyclic voltammetry characterization involves three main components: electrodes, a potentiostat, and a computer (Fig. 3). The electrodes consist of a working electrode, a reference electrode, and a counter electrode, each serving specific functions. The working electrode is a copper electrode modified with CS-GA-ZNO, the reference electrode is Ag/AgCl, and the counter electrode is platinum. These three electrodes work synergistically to ensure precise potential control and accurate current measurement during the electrochemical process [17].

The potentiostat, the primary device in this experiment, regulates the potential of the working electrode relative to the reference electrode and

measures the current generated during electrochemical reactions [18]. Data such as voltammograms are recorded and analyzed using software connected to a computer. In this study and INGENS™ Electrochemical Workstation model 1030 was used, integrated with a laptop to control parameters such as potential range, scan rate, and the number of cycles. All electrodes were immersed in a 50 ml analyte solution and connected to the potentiostat to manage the process and record the data accurately.

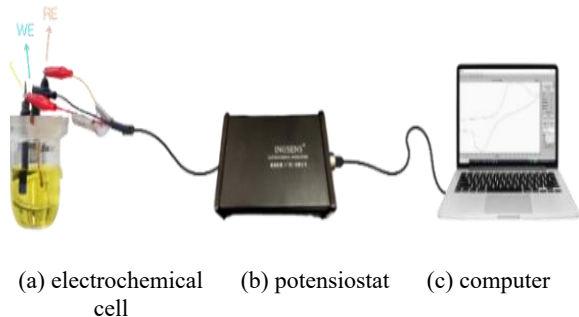


Figure 3 Cyclic voltammetry circuit illustration

### 3.2.1 Cyclic Voltammetry in 0.03 M K<sub>3</sub>[Fe(CN)<sub>6</sub>] in 0.1 M KCl

Fig. 4 presents the cyclic voltammetry measurements conducted using an analyte solution of [K<sub>3</sub>Fe(CN)<sub>6</sub>] 0.03 M in KCl 0.1 M within a potential range of -2.0 to 0.80 V, with scan rate variations of 15 mV/s, 20 mV/s, 25 mV/s, and 30 mV/s. the scan rate variations were applied to investigate the kinetics and electron transport properties of the studied electrochemical system. The resulting voltammograms exhibit quasi-reversible characteristics with well-defined oxidation and reduction peaks at all scan rates. As the scan rate increases, the electrode potential changes more rapidly, leading to faster electron transfer and an increase in both anodic (I<sub>pa</sub>) and cathodic (I<sub>pc</sub>) currents. This behavior aligns with the Randles-Sevcik equation, which states that the peak current (I<sub>p</sub>) is directly proportional to the square root of the scan rate ( $\sqrt{v}$ ) as shown in Eq. 1 [19].

$$I_p = 2,686 \times 10^5 n^{3/2} AC \sqrt{Dv} \quad (\text{Equation 1})$$

with I<sub>p</sub> is current maximum in amps, n = number of electrons transferred in the redox event (usually 1), D = diffusion coefficient in cm<sup>2</sup>/s, v = scan rate in V/s, A = electrode area in cm<sup>2</sup>, C = concentration in mol/cm<sup>3</sup>.

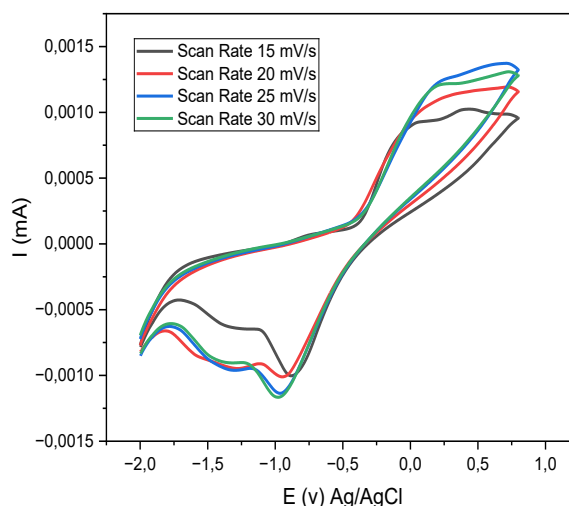


Figure 4 Cyclic Voltammogram Profile of Analyte Solution K<sub>3</sub>[Fe(CN)<sub>6</sub>] 0.03 M in KCl 0.01 M at Scan Rate Variations of 15 mV/s, 20 mV/s, 25 mV/s, and 30 mV/s

Based on the comparison of I<sub>pa</sub> and I<sub>pc</sub> values on Fig. 5, a linear correlation was obtained with an R<sup>2</sup> value of 0.8139 for anodic peak current (I<sub>pa</sub>) and 0.9524 for cathodic peak current (I<sub>pc</sub>). The regression values indicate that the system is not fully reversible, with the reduction process of ferricyanide to ferrocyanide being more efficient than the oxidation process of ferrocyanide to ferricyanide. This suggests that the reduction process is more stable compared to the oxidation process, reflecting the dynamics of electron transfer within the system. The redox chemical reaction system shown in Eq. 2-3.

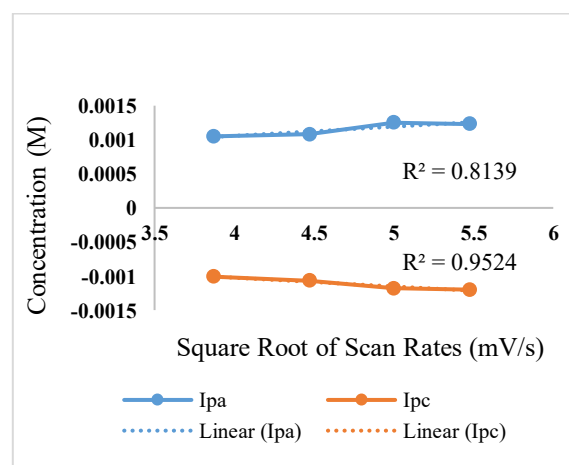
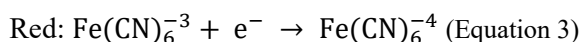
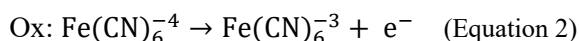


Figure 5 Comparison Chart of I<sub>pa</sub> and I<sub>pc</sub> Values of Analyte Solution K<sub>3</sub>[Fe(CN)<sub>6</sub>] 0.03 M in KCl 0.01M against ( $\sqrt{v}$ )



**Table 1** presents the ratio of anodic ( $I_{pa}$ ) and cathodic ( $I_{pc}$ ) peak currents at different scan rates. The  $I_{pa}/I_{pc}$  ratio approaches 1 across all scan rates, indicating that the electron transfer in the redox reaction occurs rapidly without significant hindrance. At a scan rate of 20 mV/s, the  $I_{pa}/I_{pc}$  ratio is 1.01, the closest to 1 compared to other scan rates. This signifies that at this scan rate, the redox process is most efficient with optimal and balanced electron transfer. This enhanced electron transfer capability is likely attributed to the modification of the working electrode surface with the CS-GA-ZnO Np/Psf nanocomposite, which improves the electrochemical properties of the electrode, as described by [20]

The  $\Delta E_p$  value (the potential difference between oxidation and reduction peaks) obtained at all scan rates exceeds 0.059 V or 59 mV. Theoretically, for a reversible redox reaction at 25 °C with  $n$  electrons involved, the ideal  $\Delta E_p$  value is  $0.0592/n$  V, or approximately 60 mV for a single electron [19]. However, in practice, this ideal value is rarely achieved due to various factors such as solution resistance, electrode surface properties, or non-fully reversible kinetic processes. When the  $\Delta E_p$  value exceeds  $0.0592/n$  V, it indicates slower electron transfer, suggesting quasi-reversible or near-reversible kinetics.

The increased  $\Delta E_p$  values indicate quasi-reversible behavior, likely due to kinetic limitations, where the electron transfer rate at the electrode surface is insufficient to maintain equilibrium between oxidized and reduced species. Additional contributing factors include surface effects such as electrode roughness or passivation layers, mass transport limitations (particularly with larger molecules like glucose) [21], and the influence of nanocomposite coatings, which may introduce interfacial barriers or modify the double-layer structure. Collectively, these factors hinder efficient charge transfer, resulting in deviations from ideal reversible redox behavior.

Moreover, the formal potential  $E^0$  denotes the midpoint potential between the centers of  $E_{pa}$  and  $E_{pc}$  [19]. The  $E^0$  obtained shows a negative value, as presented in **Table 1**. A negative  $E^0$  indicates that the electrochemical species in the analyte is more prone to oxidation than reduction. The  $E^0$  value reflects the thermodynamic tendency of the species to undergo reduction or oxidation and can be influenced by various environmental factors, such as solution pH, temperature, and the presence of other ions in the solution [22]. These findings provide valuable insights into the kinetic and thermodynamic characteristics of the redox reactions occurring in the studied electrochemical system.

**Table 1** Measurement results of cyclic voltammetry on CS-GA-ZnO Np/Psf modified copper working electrode on  $K_3[Fe(CN)_6]$  0.03 M analyte solution in KCl 0.1 M

Scan Rate (mV/s)	$E_{pa}$ (V)	$E_{pc}$ (V)	$I_{pa}$ (mA)	$I_{pc}$ (mA)	$\Delta E_p = E_{pa} - E_{pc}$ (V)	$E^0 = (E_{pa} + E_{pc})/2$ (V)	$ I_{pa}/I_{pc} $
15	0.424	-0.836	$1.05 \times 10^{-3}$	$-1.01 \times 10^{-3}$	1.260	-0.206	1.03
20	0.164	-0.968	$1.08 \times 10^{-3}$	$-1.07 \times 10^{-3}$	1.132	-0.402	1.01
25	0.224	-0.96	$1.25 \times 10^{-3}$	$-1.18 \times 10^{-3}$	1.184	-0.368	1.06
30	0.224	-0.95	$1.23 \times 10^{-3}$	$-1.20 \times 10^{-3}$	1.180	-0.366	1.02

### 3.2.2 Cyclic Voltammetry in 0.01 M Glucose in 0.1 M KCl

In addition to potassium ferricyanide solution, a glucose solution was used to evaluate the performance of the working electrode modified with CS-GA-ZnO Np/Psf nanocomposite in detecting glucose electrochemically. The analyte solution consisted of 0.01 M glucose p.a. in 0.1 M KCl, with measurements performed over a potential range of -3.5 to 2 V and scan rates of 15 mV/s, 20 mV/s, 25 mV/s, and 30 mV/s.

The cyclic voltammogram shown in **Fig. 6** indicates an increase in anodic ( $I_{pa}$ ) and cathodic ( $I_{pc}$ ) peak currents as the scan rate increased, particularly from 25 mV/s to 30 mV/s. This suggests that the electron transfer kinetics of the modified working electrode are influenced by the scan rate [23]. During the redox process, glucose is oxidized to gluconolactone, resulting in an anodic peak current ( $I_{pa}$ ), which reflects the release of electrons by glucose and their transfer through the working electrode. Subsequently, gluconolactone undergoes reduction back to glucose, producing a cathodic peak current ( $I_{pc}$ ). This process illustrates the redox mechanism

between the glucose solution and the modified electrode [24]. The redox reactions involved during cyclic voltammetry can be expressed as shown in Eq. 5-6.

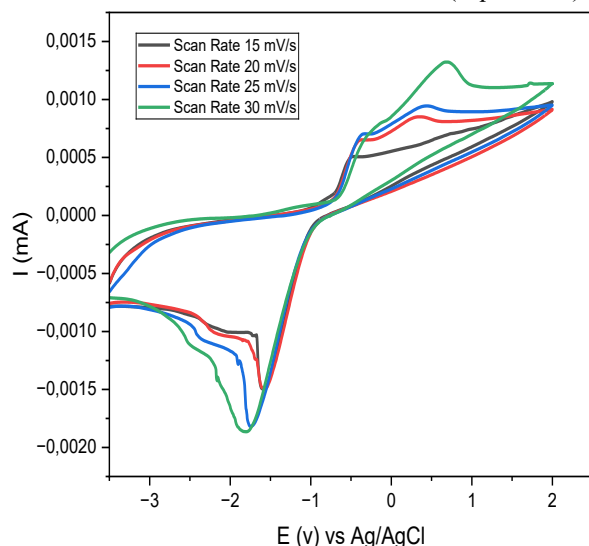
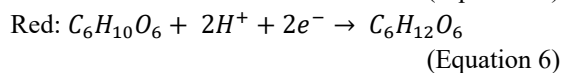
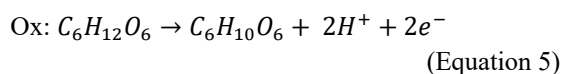


**Figure 6** Cyclic Voltammogram Profile of 0.01 M Glucose Analyte Solution in 0.01 M KCl at Scan Rate Variations of 15 mV/s, 20 mV/s, 25 mV/s, and 30 mV/s

Data presented in **Table 2** show the comparison of  $I_{pa}/I_{pc}$  ratios at various scan rates. The highest ratio was observed at a scan rate of 30 mV/s, with a value of 0.74. This indicates that electron transfer becomes more efficient at higher scan rates. According to the Randles-Sevcik equation (**Eq. 1**), the peak current ( $I_p$ ) is proportional to the square root of the scan rate ( $\sqrt{v}$ ). The  $I_{pa}/I_{pc}$  ratio of 0.74, while less than the ideal value of 1 for a reversible system, suggests quasi-reversible behavior with good redox activity, suitable for electrochemical sensing. This value reflects a favorable electrochemical response for glucose oxidation, supported by the nanocomposite's enhanced conductivity and surface area. Therefore, an increase in scan rate not only enhances  $I_{pa}$  and  $I_{pc}$  values but also reflects the excellent electrochemical response of the modified electrode toward glucose detection. Glucose has a relatively large molecular structure, making the diffusion rate in the solution a critical factor influencing the efficiency of electron transfer processes during electrochemical reactions [21]. To accelerate chemical transfer and enhance electrochemical response, a higher diffusion rate is required. This can be achieved by optimizing several parameters, one of which is the scan rate.

**Table 2** Measurement results of cyclic voltammetry on CS-GA-ZnO Np/Psf modified copper working electrode on 0.01 M glucose p.a analyte solution in 0.1 M KCl

Scan Rate (mV/s)	$E_{pa}$ (V)	$E_{pc}$ (V)	$I_{pa}$ (mA)	$I_{pc}$ (mA)	$\Delta E_p = E_{pa} - E_{pc}$ (V)	$E_0 = (E_{pa} + E_{pc})/2$ (V)	$ I_{pa}/I_{pc} $
15	0.720	-1.564	$7.20 \times 10^{-4}$	$-1.48 \times 10^{-3}$	2.284	0.360	0.47
20	0.364	-1.548	$8.50 \times 10^{-4}$	$-1.49 \times 10^{-3}$	1.912	0.182	0.57
25	0.452	-1.728	$9.44 \times 10^{-4}$	$-1.81 \times 10^{-3}$	2.180	0.226	0.52
30	0.688	-1.710	$1.32 \times 10^{-3}$	$-1.78 \times 10^{-3}$	2.380	0.334	0.74

Comparatively, previous research [24] demonstrated ratios  $>1$  for chitosan-modified electrodes, highlighting the role of electrode material in enhancing reversibility. The lower ratio (0.74) in this study may reflect unoptimized surface kinetics or diffusion constraints that deviations from ideality ( $I_{pa}/I_{pc} = 1$ ) often arise from adsorption or slow heterogeneous electron transfer. To improve sensor performance, future work could optimize scan rates or modify the electrode surface to accelerate glucose diffusion and electron transfer, thereby achieving higher sensitivity and reversibility.

The oxidation-reduction peak potential difference ( $\Delta E_p > 0.0592/n$  V) confirms quasi-

reversible character in the electrochemical process. This higher  $\Delta E_p$  value suggests the presence of kinetic barriers in the electron transfer process during the redox reaction. This condition is also influenced by the number of electrons transferred in the glucose redox process, where a larger number of electrons tends to slow down the electron transfer, especially for large molecules like glucose.

Additionally, the formal potential ( $E^0$ ) values obtained are entirely positive. This indicates that the electrochemical species in the analyte, specifically glucose, are more prone to oxidation than reduction. A positive potential reflects that the oxidation process, in which glucose donates

electrons to form gluconolactone, is more dominant and energetically favorable. The  $E^\circ$  value is also influenced by the electrochemical environment, including the solution's pH and the properties of the electrode surface used. These factors collectively describe the complex dynamics of electron transfer in the electrochemical measurement of glucose.

Fig. 7 shows a graph comparing  $I_{pa}$  and  $I_{pc}$  values. The linear correlation for anodic peak current ( $I_{pa}$ ) had an  $R^2$  value of 0.8713, while the cathodic peak current ( $I_{pc}$ ) had an  $R^2$  value of 0.7709. These  $R^2$  values indicate that the oxidation of glucose to gluconolactone is more efficient and stable than the reduction of gluconolactone back to glucose. This finding demonstrates that the CS-GA-ZnO Np/Psf-modified electrode provides a stable and consistent electrochemical response for glucose detection across different scan rates.

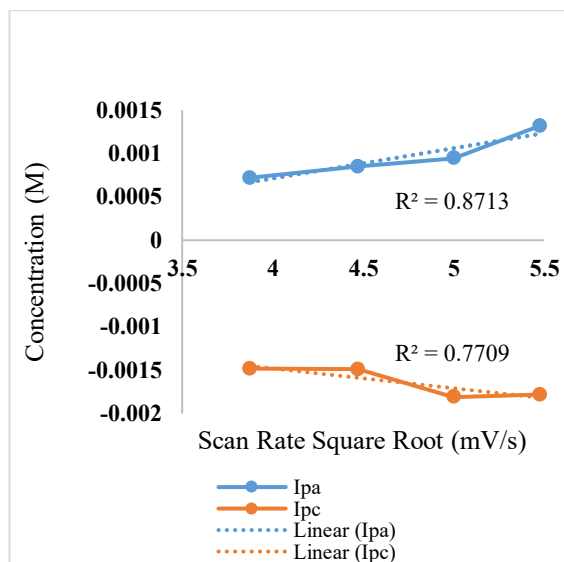


Figure 7 Comparison Chart of  $I_{pa}/I_{pc}$  Value of 0.01 M Glucose Analyte Solution in 0.01M KCl

Table 3 Infrared (IR) Spectral Analysis of Functional Groups in the CS-GA-ZnO Np/Psf Nanocomposite-Modified Copper Electrode and Their Contribution to Electrochemical Stability

Functional Group/Bond	Type of Vibrations	Nanocomposite Wavenumber ( $\text{cm}^{-1}$ )	Reference Wavenumber ( $\text{cm}^{-1}$ )
O-H	Stretching	3442	3478 [27]
N-H	Stretching	3442	3458 [28]
C-H aliphatic	Stretching	2964 and 2887	2925 [29]
CH=N	Stretching	1643	1610-1635 [30]
SO <sub>2</sub>	Stretching	1307 and 1263	1000-1300
C-O-C	Stretching	1151, 1114, and 1058	1153 and 1066 [31]
C-H aliphatic	Bending (Out-of-Plane)	721	720-725

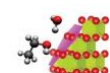
### 3.3 Characterization of CS-GA-ZnO Np/Psf-Modified Copper Electrodes Using FTIR

The FTIR spectrum of the CS-GA-ZnO Np/Psf nanocomposite exhibits a combination of characteristic peaks from its constituent components, namely chitosan (CS), glutaraldehyde (GA), polysulfone (Psf), and ZnO nanoparticles. In the nanocomposite spectrum, a distinctive peak at  $3442 \text{ cm}^{-1}$  corresponds to the overlapping vibrations of hydroxyl (O-H) and amine (N-H) groups [25]. The intensity of this Peak decreases compared to the pure chitosan spectrum, indicating the formation of hydrogen bonds between the O-H and N-H groups of chitosan and the carbonyl groups of glutaraldehyde or the oxide groups of ZnO Np.

Other peaks at  $2964 \text{ cm}^{-1}$  and  $2887 \text{ cm}^{-1}$  represent the aliphatic C-H bond vibrations, indicating the presence of glutaraldehyde and NMP, where NMP acts as the solvent for

polysulfone [32]. At  $1643 \text{ cm}^{-1}$ , the spectrum shows a distinctive peak associated with the crosslinking process between chitosan and glutaraldehyde [5]. This involves the reaction of chitosan's amine groups with the carbonyl groups of glutaraldehyde, forming imine bonds (CH=N) [30]. This vibration value falls within the range for Schiff base (-C=N-) vibrations, reported at  $1620\text{-}1660 \text{ cm}^{-1}$  in the book *Spectrometric Identification of Organic Compounds* [26].

In the nanocomposite spectrum, peaks at  $1307 \text{ cm}^{-1}$  and  $1263 \text{ cm}^{-1}$ , characteristic of sulfone (SO<sub>2</sub>) group vibrations in polysulfone, remain present but show slight changes in intensity [33]. Additionally, peak in the range of  $1150\text{-}1058 \text{ cm}^{-1}$ , representing glycosidic bond (C-O-C) vibrations from the basic structures of chitosan and polysulfone, are observed in the nanocomposite spectrum. This indicates the retention of the main polymer structure despite



modifications [16]. A peak at  $721\text{ cm}^{-1}$  corresponds to aliphatic C-H bond vibrations [25], which are also part of the chitosan structure. Overall, the FTIR spectrum confirms the successful formation of the CS-GA-ZnO Np/Psf nanocomposite with significant chemical interactions between its components.

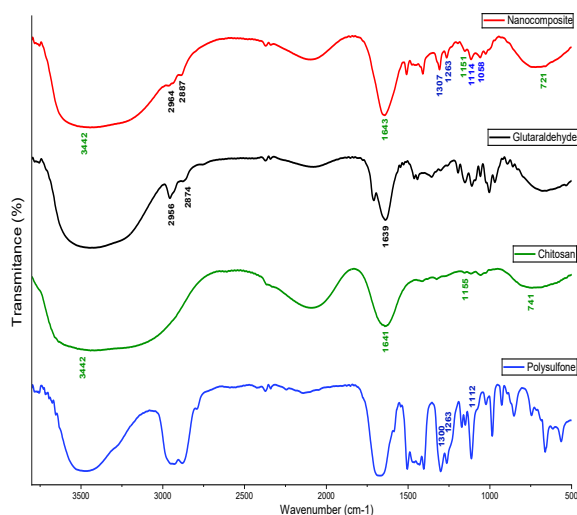


**Figure 8** The FTIR spectra of the CS-GA-ZnO Np/Psf nanocomposite were compared with its components GA, chitosan, and Psf.

#### 4 Conclusion

This study successfully developed a chitosan-glutaraldehyde-ZnO nanoparticle/polysulfone (CS-GA-ZnO Np/Psf) nanocomposite for modifying copper electrodes, aimed at enhancing electrochemical performance. Electrochemical analysis revealed that the modified electrode exhibited near-reversible electron transfer behavior in the ferricyanide system, with an  $I_{pa}/I_{pc}$  ratio close to 1, although  $\Delta E_p$  values indicated quasi-reversible kinetics. For glucose, the electrode demonstrated improved electron transfer efficiency at higher scan rates, despite slower kinetics due to glucose's larger molecular size, as reflected in positive  $E^\circ$  values. FTIR characterization confirmed the successful formation and stability of the nanocomposite, with key functional groups identified, including O-H and N-H stretching (hydrogen bonding), C=N stretching (imine bond formation), and asymmetric/symmetric S=O stretching (sulfone groups). The presence of ether (C-O-C) and aliphatic C-H out-of-plane bending further validated the composite's structural integrity. These results highlight the potential of the modified electrode for detecting analytes with

diverse redox properties and molecular structures, offering promising applications in electrochemical sensing.

#### Acknowledgement

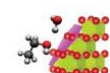
This work was supported by the Ministry of Education, Culture, Research, and Technology through the Master's Thesis Research (PTM) grant under Main Contract No. DRTPM-LLDIKTI 106/E5/PG.02.00.PL/2024 (June 11, 2024), and Derived Contracts No. 016/SP2H/RT-MONO/LL4/2024 (June 14, 2024) and No. 002/SPK/LPPMUNJANI/VI/2024 (June 19, 2024).

#### References

- [1] Biała K., Moschou D., Marken F., & Estrela P., 2022, Electrochemical sensors based on metal nanoparticles with biocatalytic activity, *Microchimica Acta*, 189: 1-20. <https://doi.org/10.1007/s00604-022-05252-2>
- [2] Negm NA., Abubshait HA., Abubshait SA., Abou Kana MT., Mohamed EA., & Betiha MM., 2020, Performance of chitosan polymer as platform during sensors fabrication and sensing applications, *International Journal of Biological Macromolecules*, 165, 402-435. <https://doi.org/10.1016/j.ijbiomac.2020.09.130>
- [3] Murniati A., Shardi S., Fauzi I., Hardian A., ... Jasmansyah, 2022, Immobilization of Crude Polyphenol Oxidase Purple Eggplant Extract on Chitosanmembrane For For Removal of Phenol Wastewater, *European Chemical Bulletin*, 11: 117-125. <http://dx.doi.org/10.31838/ecb/2022.11.10.016>
- [4] Karrat A., & Amine A., 2020, Recent advances in chitosan-based electrochemical sensors and biosensors, *Arab. J. Chem. Environ. Res*, 7(2), 66-93.
- [5] Murniati A., Nur IH., Gumelar N., Budiman S., Buchari B., Gandasmita S., & Nurachman Z., 2024, Evaluation of Scan Rate Influence on Cyclic Voltammograms of Copper Electrodes Coated with PS-CS-GA/ZnO Nanocomposite, *Jurnal Kartika Kimia*, 7(1), 56-63. <https://doi.org/10.26874/jkk.v7i1.256>
- [6] Liu P., & Yin L., 2020, Application of glassy carbon electrode modified with chitosan and ZnO nanoparticles as enzymatic glucose biosensor, *International Journal of Electrochemical Science*, 15(6), 5821-5832. <https://doi.org/10.20964/2020.06.67>



- [7] Aprillianti RN., Rahayu M., Hardian A., & Murniati A., 2024, Effect of Polyethylene Glycol Concentration on the Structural and Mechanical Properties of Polysulfone-Based Membrane, *Journal of Chemistry and Environment*, 25-38. <http://dx.doi.org/10.56946/jce.v3i2.469>
- [8] Reddy N., Reddy R., & Jiang Q., 2015, Crosslinking biopolymers for biomedical applications, *Trends in biotechnology*, 33(6), 362-369. <https://doi.org/10.1016/j.tibtech.2015.03.008>
- [9] Murniati A., Buchari B., Gandasmita S., & Nurachman Z., 2018, Sintesis dan Karakterisasi Polipirol pada Elektroda Kerja Kasa Baja dengan Metode Voltametri Siklik, *Jurnal Sains Materi Indonesia*, 13(3), 210-215. <http://dx.doi.org/10.17146/jsmi.2012.13.3.4674>
- [10] Murniati A., Buchari B., Gandasmita S., & Nurachman Z., 2012, Synthesis and characterization of polypyrrole polyphenol oxidase (PPy/PPO) on platinum electrode, *Research Journal of Pharmaceutical, Biological and Chemical Sciences*, 3, 855-864.
- [11] Gunawan AF., Hardian A., & Murniati A., 2025, Cyclic Voltammetry Study of the Influence of Concentration of K3 [Fe (CN) 6] and Glucose on Glassy Carbon Electrode, *ALCHEMY Jurnal Penelitian Kimia*, 21(1), 43-52. <https://dx.doi.org/10.20961/alchemy.21.1.87604.43-52>
- [12] Hasnidawani JN., Azlina HN., Norita H., Bonnia NN., Ratim S., & Ali ES., 2016, Synthesis of ZnO nanostructures using sol-gel method, *Procedia chemistry*, 19, 211-216. <https://doi.org/10.1016/j.proche.2016.03.095>
- [13] Nasution Z., Agusnar H., Alfian Z., & Wirjosentono B., 2013, Pengaruh viskositas kitosan dari berbagai berat molekul terhadap pembuatan kitosan nanopartikel menggunakan ultrasonic bath, *Jurnal Teknologi Kimia Unimal*, 2(2), 68-79.
- [14] Józwiak T., Filipkowska U., Szymczyk P., Rodziewicz J., & Mielcarek A., 2017, Effect of ionic and covalent crosslinking agents on properties of chitosan beads and sorption effectiveness of Reactive Black 5 dye, *Reactive and Functional Polymers*, 114, 58-74. <https://doi.org/10.1016/j.reactfunctpolym.2017.03.007>
- [15] Kildeeva NR., Perminov PA., Vladimirov LV., Novikov VV., & Mikhailov SN., 2009, About mechanism of chitosan cross-linking with glutaraldehyde, *Russian journal of bioorganic chemistry*, 35, 360-369.
- [16] Islam N., Dmour I., Taha MO., 2019, Degradability of chitosan micro/nanoparticles for pulmonary drug delivery, *Heliyon*, 5(5), 1-9. <https://doi.org/10.1016/j.heliyon.2019.e01684>
- [17] Elgrishi N., Rountree KJ., McCarthy BD., Rountree ES., Eisenhart TT., & Dempsey JL., 2018, A practical beginner's guide to cyclic voltammetry, *Journal of chemical education*, 95(2), 197-206. <https://doi.org/10.1021/acs.jchemed.7b00361>
- [18] Azmi NH., Nordin AN., Suhaimi MI., Ming LL., ... Raghieb M., 2024, Flexible Potentiostat Readout Circuit for Electrochemical Sensors, *Indonesian Journal of Electrical Engineering and Informatics (IJEI)*, 12(2), 333-343. <http://dx.doi.org/10.52549/ijeai.v12i2.5520>
- [19] Yamada H., Yoshii K., Asahi M., Chiku M., & Kitazumi Y., 2022, Cyclic voltammetry part 1: Fundamentals, *Electrochemistry*, 90(10), 102005-102005. <https://doi.org/10.5796/electrochemistry.22-66082>
- [20] Kounaves SP. Voltammetric Techniques. In: *Handbook Of Instrumental Techniques for Analytical Chemistry*. 2000, Pp. 709–726.
- [21] Miyamoto S., & Shimono K., 2020, Molecular Modeling to Estimate the Diffusion Coefficients of Drugs and Other Small Molecules, *Molecules*, 25(22):1-8. <https://doi.org/10.3390/Molecules25225340>
- [22] Nimmo M. *Differential Pulse Polarography and Voltammetry*. Springer, 1991.
- [23] Espinoza EM., Clark JA., Soliman J., Derr JB., Morales M., & Vullev VI., 2019, Practical aspects of cyclic voltammetry: how to estimate reduction potentials when irreversibility prevails, *Journal of The Electrochemical Society*, 166(5), H3175-H3187. <https://orcid.org/0000-0002-3416-9686>
- [24] Chen H., Gu T., Lv L., Chen X., Lu Q., Kotb A., & Chen W., 2024, A Biocompatible, Highly Sensitive, and Non-Enzymatic Glucose Electrochemical Sensor Based on a Copper-Cysteamine (Cu-Cy)/Chitosan-Modified Electrode, *Nanomaterials*, 14(17), 1430. <https://orcid.org/10.3390/Nano14171430>
- [25] Fatoni A., Hariani PL., Hermansyah H., & Lesbani A., 2018, Synthesis and characterization of chitosan linked by



- methylene bridge and schiff base of 4, 4-diaminodiphenyl ether-vanillin, *Indonesian Journal of Chemistry*, 18(1), 92-101. <https://doi.org/10.22146/ijc.25866>
- [26] Silverstain RM., Webster FX., Kiemle DJ. *Spectrometric Identification of Organic Compounds*. 7th ed. New York: John Wiley & Sons, Inc, 2005.
- [27] Yasmeen S., Kabiraz MK., Saha B., Qadir MD., Gafur MD., & Masum S., 2016, Chromium (VI) ions removal from tannery effluent using chitosan-microcrystalline cellulose composite as adsorbent, *Int. Res. J. Pure Appl. Chem*, 10(4), 1-14. <http://dx.doi.org/10.9734/IRJPAC/2016/23315>
- [28] Varma R., Pratihari A., Pasumpon N., & Vasudevan S., 2022, Extraction and Characterization of Chitosan from the Cuttlebone of Spineless Cuttlefish, *Sepiella inermis*, *Mater. Int.*, 4(4), 1-10. <https://doi.org/10.33263/Materials44.002>
- [29] Li B., Shan CL., Zhou Q., Fang Y., Wang YL., ... & Sun GC., 2013, Synthesis, characterization, and antibacterial activity of cross-linked chitosan-glutaraldehyde, *Marine drugs*, 11(5), 1534-1552. <https://doi.org/10.3390/md11051534>
- [30] Rohini R., Reddy PM., Shanker K., Kanthaiah K., Ravinder V., & Hu A., 2011, Synthesis of mono, bis-2-(2-arylideneaminophenyl) indole azomethines as potential antimicrobial agents, *Archives of pharmacal research*, 34, 1077-1084.
- [31] Queiroz MF., Teodosio Melo KR., Sabry DA., Sassaki GL., & Rocha HAO., 2015, Does the use of chitosan contribute to oxalate kidney stone formation?, *Marine drugs*, 13(1), 141-158. <https://doi.org/10.3390/md13010141>
- [32] Nandiyanto ABD., Ragadhita R., & Fiandini M., 2023, Interpretation of Fourier transform infrared spectra (FTIR): A practical approach in the polymer/plastic thermal decomposition, *Indonesian Journal of Science and Technology*, 8(1), 113-126. <http://dx.doi.org/10.17509/ijost.v8i1.53297>
- [33] Nguyen HTV., Ngo THA., Do KD., ... Vu TA., 2019, Preparation and characterization of a hydrophilic polysulfone membrane using graphene oxide, *Journal of Chemistry*, 1-10. <https://doi.org/10.1155/2019/3164373>

